PHYSICAL REVIEW D **96**, 024001 (2017)

# Entropy production due to Lorentz invariance violation

Hosein Mohammadzadeh, Mehrnoosh Farahmand, and Mahnaz Maleki
*Department of Physics, University of Mohaghegh Ardabili, P.O. Box 179, Ardabil, Iran*
(Received 4 September 2016; published 6 July 2017)

It is generally believed that the concept of the spacetime continuum should be modified for distances as small as the Planck length. This is a length scale at which the spacetime might have a discrete structure and quantum gravity effects are dominant. Presumably, the microscopic fluctuations within the geometry of spacetime should result in an enormous entropy production. In the present work, we look for the effects of Lorentz invariance violation (LIV) in flat and curved backgrounds that can be measured by quantum entanglement and quantum thermodynamic entropies for scalar modes. Our results show that the general behavior of these entropies is the same. We also consider variations of the entropies with respect to LIV and cosmological and field parameters. Using the properties of these entropies, along with detecting the most entangled modes, we extract information about the past existence of LIV, which in turn might be useful in recovering the quantum structure of gravity. Indeed, the occurrence of a peak in the behavior of these entropies for a specific momentum could provide information about the expansion parameters. Moreover, information about the LIV parameter is codified in this peak.

DOI: 10.1103/PhysRevD.96.024001

## I. INTRODUCTION

According to the Lorentz invariance condition, which is the cornerstone of the theory of special relativity (SR), the spacetime appears to be the same at all length scales. However, classical general relativity (GR), which extends SR to include gravity and accelerated motions, predicts the formation of singularities (such as the big-bang singularity) in the fabric of spacetime that must be eventually removed. These are superdense regions of extreme gravity where the classical GR breaks down and quantum gravity may take over in such regimes to resolve the classical spacetime singularity. Different approaches to quantum gravity have been developed within various contexts such as string theory [1,2] and loop quantum gravity [3,4]. However, some approaches to quantum gravity propose that a microscopic structure of spacetime may lead to Lorentz symmetry violation. The violation of such a condition has been studied in noncommutative geometry [5,6] and theories with extra dimensions [7], as well as in the context of the discretization process. The effects of quantum gravity are important near the Planck scale. Studies in the field of trans-Planckian physics on the Hawking effect and inflationary cosmology have employed scalar fields with high frequency dispersion to investigate the role of short distance physics on the behavior of a quantum field. As we know, the energy and momentum quantities for a particle, as related to each other by a dispersion relation, would change under Lorentz transformation, in such a way that the standard dispersion relation remains invariant. However, it is generally believed that within the regimes where the structure of spacetime becomes dominated by quantum effects, the smallest length scale can modify the standard dispersion relation so that the discrete nature of space at short distances can produce a modified dispersion relation with an extra term that induces violation of Lorentz invariance [8–16]. In this regard, there is evidence showing that this symmetry becomes broken in some phenomena [17–22]. The effects of LIV have been discussed in inflationary cosmology, the dark energy problem, and baryogenesis [23–28].

In the model herein, we apply corrections (at the quantum scale) to initial conditions of an early Universe in order to explore the dynamics of spacetime and to understand the physical properties of the Universe. We would like to explain the mechanisms that govern the transition from a highly quantum correlated field state to the current classical background. This is the assumption of the quantum-to-classical transition produced by a quantum gravitational vacuum; in other words, particles are only some excitations of the quantum gravity vacuum. Indeed, particle-filled states are given by taking the semiclassical limits of the quantum gravity vacuum. LIV in the vacuum of the early Universe can lead to the creation of particles which occurs in the absence of LIV. in the late Universe. Accordingly, the quantum structure of geometry causes the existence of particles. A field theory in flat spacetime will naturally concentrate on perturbations around a natural vacuum state. Therefore, a dynamic LIV model can explain the mechanism of particle creation in flat spacetime. However, in curved spacetime, the effects of spacetime on the field are important. Particle creation is an interesting prediction of quantum field theory in curved spacetime [29]. Particles are produced by propagation of a quantum field through an expanding Universe. However, if a spacetime is conformally equivalent to Minkowski spacetime, then a conformally invariant field, propagating in such spacetime, does not produce particles. Field equations

 © 2017 American Physical Society

in the quantum field theory in curved spacetime are locally Lorentz invariant. By adding a term to the field equation, the conformal invariance is broken and such particles are generated. The effects of LIV on particle creation have been studied in [30,31]. Particle generation, after conformal symmetry breaking, produces entanglement in the final states of the field.

According to the above, the structure of the present Universe is classical and occurrence of this transition needs to be understood [32]. All structures of the Universe can be traced back to primordial quantum fluctuations during an accelerated expansion phase of the early Universe. It is understood that the quantum nature of fluctuations is not lost as long as the system is an entangled state. Therefore, it is appropriate to explain the appearance of the classical nature in the state of entanglement in order to understand the mechanism of the quantum-to-classical transition in primordial fluctuations. Zero entanglement was found in the Universe between two spatially separated regions when their physical separation was more than that of the Hubble horizon. Therefore, long-wavelength quantum fluctuations can be treated as classical fluctuations [33].

Entanglement is applied as an important tool in quantum information theory. It plays a central role in black hole thermodynamics [34–41], as well as in the information loss problem [42–47]. Recently, entanglement and quantum information techniques have been investigated to learn about certain aspects of gravity and black hole physics [48–53] in an expanding Universe [54–69]. Recent efforts have shown that the dynamics of spacetime can generate entanglement. In fact, the energy content of the early Universe was dominated by an entangled quantum field background. If the effects of such an entanglement do survive, through a weakly interacting field, until our present Universe, they can provide precise information about the nature of the early Universe and the history of spacetime. The extraction of this entanglement enables us to deduce cosmological parameters of the underlying spacetime. However, it has been difficult to observe practically the effects of entanglement in the context of experimental cosmology. A method of deducing cosmological parameters of the spacetime through this entanglement that emerge via gravitational interactions could intuitively give new insights into the early Universe [56–58]. This has benefited researchers concerned with entanglement in the thermodynamic properties of spacetime [70] and spacetime fluctuations [71]. Theoretical cosmology must cover entanglement as a purely quantum effect with a fundamental role in the thermodynamic properties of Friedmann-Robertson-Walker (FRW) spacetime [70]. Observational cosmology can search for witnesses for purely quantum effects in the early Universe. In addition, there are laboratory analogies that use the quantum effect in analogue curved spacetimes to study entanglement [56]. In these experimental setups of analogue models using Bose-Einstein condensates or ion traps and detectors, entanglement can be measured directly.

Entanglement is an observer-dependent quantity and decreases from the viewpoint of an accelerated observer in flat spacetime [72]. Despite differences between entanglements generated by scalar and spinor fields, entanglement in curved spacetime or by dynamics of the underlying spacetime might not be invariant [54,55,68]. Usually, von Neumann entropy is used to describe entanglement.

Thermodynamics is employed as a powerful tool in cosmology. Recently, interesting results show that the inner friction stemming from the quantum fluctuations of the field plays a significant role in increasing entropy in the Universe [73]. It has been established that the thermodynamical properties of entanglement entropy, obtained from quantum information theory, have similarities with the results of the quantum thermodynamic entropy of spacetime. The difference between these two entropies shows that particle creation entropy can be rescaled to entanglement entropy [74].

We study the effects of LIV on entanglement generation and particle creation entropy for both flat and curved backgrounds. Our interest is to investigate properties of a scalar field. For this goal, attention is given to a free scalar field on a spatial lattice. The discreteness effect of spacetime on dispersion relation is analyzed leading to LIV. Therefore, we consider particle creation and generated entanglement due to LIV during the evolution of spacetime. In other words, we make use of a time-dependent parameter to look for effects of dynamical LIV on the appearance of entanglement and entropy production in flat spacetime. Also, we consider the LIV process and its effects on entanglement and entropy production of an expanding Universe. Contrary to the flat case, we take advantage of the LIV in the context of the evolution of spacetime itself in curved spacetime. An approach has been presented in [73]. The aforementioned approach is applied to evaluate particle creation entropy and von Neumann entropy in order to determine entanglement.

This paper is organized as follows. In Sec. II we extract LIV in terms of the dispersion relation from a discrete spacetime. In Sec. III we present scalar field quantization in flat spacetime. In Sec. IV we introduce the LIV model in flat spacetime and obtain a state of particle creation. Section V deals with deriving entanglement and particle creation entropies. In Sec. VI the behavior of entanglement and thermodynamic entropies in flat spacetime is investigated in more detail. In Sec. VII, we define an expanding spacetime and probe the effects of quantizing the LIV model on this spacetime. We then proceed to investigate, in detail, the behavior of entanglement and thermodynamic entropies for this spacetime. Finally, a summary of the main results of our work is presented in Sec. IX.

## II. SCALAR FIELD ON A DISCRETE SPACETIME

We consider a free scalar field evolving on a spatial lattice with continuous time. The Klein-Gordon equation then reads [75]

$$\ddot{\phi} = \nabla^2\phi - m^2\phi, \tag{1}$$

where $m$ is mass of the particle. Equation (1) exhibits the standard dispersion relation for energy-momentum of the particle given by

$$\omega^2 = \mathbf{k}^2 + m^2. \tag{2}$$

We can rewrite the Laplacian term in Eq. (1) on a spatial lattice as follows:

$$\begin{aligned}\sigma^2\nabla^2\phi &\to \phi(\mathbf{n}+\boldsymbol{\sigma}) + \phi(\mathbf{n}-\boldsymbol{\sigma}) - 2\phi(\mathbf{n}) \\ &= (\mathbf{d}^+ + \mathbf{d}^- - 2)\phi(\mathbf{n}),\end{aligned} \tag{3}$$

where the three-dimensional vector $\mathbf{n} \equiv \sigma(n_1, n_2, n_3)$; $\boldsymbol{\sigma} \equiv \sigma(1,1,1)$; $\sigma$ is the lattice spacing; and $\mathbf{d}^{\pm}\phi(\mathbf{n}) = \phi(\mathbf{n} \pm \boldsymbol{\sigma})$ are the shift operators. Thus, the lattice Klein-Gordon equation can be found as

$$\ddot{\phi} = \frac{(\mathbf{d}^+ + \mathbf{d}^- - 2)}{\sigma^2}\phi - m^2\phi. \tag{4}$$

The natural solution to Eq. (4) is

$$\phi = e^{i(\mathbf{k}.\mathbf{n}+\omega t)}. \tag{5}$$

Substituting the above solution into Eq. (4), we get, within the interval $-\pi < \mathbf{k}.\boldsymbol{\sigma} < \pi$,

$$-\omega^2\phi = \frac{e^{i\mathbf{k}.\boldsymbol{\sigma}} + e^{-i\mathbf{k}.\boldsymbol{\sigma}} - 2}{\sigma^2}\phi - m^2\phi. \tag{6}$$

Therefore, the dispersion relation for the lattice model takes the following form:

$$\omega^2 = m^2 - \frac{2}{\sigma^2}(\cos\mathbf{k}.\boldsymbol{\sigma} - 1). \tag{7}$$

We note that Eq. (7) is not invariant under Lorentz transformation. For the low-energy particle ($\mathbf{k}.\boldsymbol{\sigma} \ll 1$) we have

$$\omega^2 = m^2 + k^2 - \mathcal{O}(k^4\sigma^2), \tag{8}$$

where $k = |\mathbf{k}|$. Equation (8) implies that, in the continuous limit where $\sigma \to 0$ standard dispersion relation, Eq. (2) is recovered.

Quantum gravity effects modify the standard dispersion to include an extra term as a LIV term [76]. Thus, the modified dispersion relation is found as

$$\omega^2 = m^2 + k^2 - \sigma^2 k^4, \tag{9}$$

where the last term breaks the Lorentz symmetry. Here, the parameter $\sigma^2$ is called the LIV coefficient, which is naturally expected to be proportional to the Planck length $l_P$. The above relation gives the semiclassical limit beyond the standard model, such that if we adopt $l_P \to 0$, we arrive at the standard form of the dispersion relation.

## III. FIELD QUANTIZATION IN A FLAT SPACETIME

Let us consider a Minkowskian spacetime. In this case the spacetime admits a global timelike Killing vector field. The existence of such a Killing vector is necessary, since it allows for a meaningful definition of particle states. Thus, we classify solutions according to the Klein-Gordon equation into positive and negative frequency modes. Modes of the plane wave are chosen using symmetries of the Minkowskian spacetime, i.e., $\{\tilde{u}_k, \tilde{u}_k^*\} \propto e^{\pm i\mathbf{k}.\mathbf{x}}e^{\pm i\tilde{\omega}t}$, as a basis to expand the field in terms of these modes such that $\tilde{\omega}^2 = k^2 + m^2$. This basis allows us to distinguish between positive and negative frequencies. Therefore, the field quantization can be done in terms of these modes,

$$\phi(t,x) = \int d\mathbf{k}[\tilde{a}_k\tilde{u}_k(t,x) + \tilde{a}_k^\dagger\tilde{u}_k^*(t,x)], \tag{10}$$

where coefficients of the expansion are interpreted as creation and annihilation operators, $\tilde{a}_k^\dagger$, $\tilde{a}_k$, which satisfy the commutation relations $[\tilde{a}_k^\dagger, \tilde{a}_k] = \delta_{k,k'}$. We notice that the basis modes are not unique. There are generally other choices for such sets with the properties of the original modes. The preference of one set of solutions is that it depends on what is lost in the transition from the initial situation to the final one. The vacuum state and number of observed particles depend on the selected set. An alternative set of modes, $\{u_k, u_k^*\}$, can be chosen to form a complete basis in order to expand the field as

$$\phi(t,x) = \int d\mathbf{k}[a_k u_k(t,x) + a_k^\dagger u_k^*(t,x)], \tag{11}$$

where according to the previous set, $a_k^\dagger$ and $a_k$ are the creation and annihilation operators in the new basis with the commutation relations $[a_k^\dagger, a_k] = \delta_{k,k'}$. Using the inner product, one obtains a transformation between the mode solutions as

$$\tilde{u}_k(t,x) = \alpha_k u_k(t,x) + \beta_k u_{-k}^*(t,x), \tag{12}$$

which accordingly implies a transformation between the creation and annihilation operators as

$$\tilde{a}_k(t,x) = \alpha_k a_k(t,x) - \beta_k a_{-k}^\dagger(t,x), \tag{13}$$

where $\alpha_k$ and $\beta_k$ represent the Bogoliubov coefficients. It is worth mentioning that we refer to initial and final operators as "in" and "out," respectively, and we denote all quantities related to the in region using a tilde, and those related to the out region without a tilde. The canonical relations give rise to

$$|\alpha_k|^2 - |\beta_k|^2 = 1. \tag{14}$$

Now, consider the system being in the vacuum state in "in-modes"; the expectation value of the out-number operator is evaluated in the in-vacuum to determine how many particles are detected by the "out-mode" as

$$\langle N_k\rangle = \langle \tilde{0}_k | a_k^\dagger a_k | \tilde{0}_k\rangle = |\beta_k|^2. \tag{15}$$

Therefore, the observed number of particles with respect to the set of out-modes, which depend on Bogoliubov coefficients, will disagree with the vacuum state of the in-modes, as long as one of the Bogoliubov coefficients $\beta_k$ is nonzero. This is consistent with the scenarios of quantum field theory in curved spacetime [29].

## IV. LORENTZ VIOLATION IN THE FLAT SPACETIME

Let us begin with the modified dispersion relation Eq. (9). An appropriate Lagrangian to reach Eq. (9) for a scalar field, $\phi$, is given by

$$\mathcal{L} = \frac{1}{2}[\partial^\mu\phi\partial_\mu\phi - m^2\phi^2 + \sigma^2(D^2\phi)^2], \tag{16}$$

where $D^2$ is known as the spatial Laplacian defined as

$$D^2\phi = -D^\mu D_\mu\phi = -q^{\mu\nu}\partial_\nu(q_\mu^\tau\partial_\tau\phi). \tag{17}$$

Here $q_{\mu\nu}$ indicates the spatial metric orthogonal to the unit timelike vector $u^\mu$ as

$$q_{\mu\nu} = -\eta_{\mu\nu} + u_\mu u_\nu, \qquad \eta^{\mu\nu}u_\mu u_\nu = 1. \tag{18}$$

The aether is taken as a coordinate system which exhibits constant $u^\mu$ and $u^\mu$ is denoted as the four-vector velocity of an inertial observer, whose aether is his rest frame. We then have $u^\mu = (1,0,0,0)$ in the rest frame. The equation of motion for $\phi$ can be obtained by equating the variation of the action, $S = \int \mathcal{L}d^4x$, to zero with respect to $\phi$ which leads to

$$[\partial_t^2 - \partial_{\mathbf{x}}^2 + m^2 - \sigma^2\partial_{\mathbf{x}}^4]\phi = 0. \tag{19}$$

Since there is a global timelike Killing vector field, we are allowed to select solutions to Eq. (19) separated into time-dependent and space-dependent parts as $u(t,x) = e^{i\mathbf{k}.\mathbf{x}}T_k(t)$. Therefore, Eq. (19) is reduced to

$$[\partial_t^2 - k^2 + m^2 - \sigma^2k^4]T_k(t) = 0. \tag{20}$$

The LIV effects are expected to appear at early time and then entirely subside at late time. Thus, we choose a time-dependent LIV parameter such that its dynamical behavior is in accordance with its behavior at early and late times. In other words, the LIV parameter for the early time will have a constant value and for the late time will vanish,

$$\sigma^2(t) = \frac{\sigma_0^2}{1+e^{\delta_0 t}}, \tag{21}$$

where $\sigma_0$ denotes the initial value of the LIV parameter stemming from the effects of the early quantum gravity regime and $\delta_0$ is the rate of reduction of the effects of LIV.

This form of the time evolution is chosen such that the resulting equations are exactly solvable, although other functionalities for the LIV parameter can be found that could possibly be consistent with the above situations. The origin of the dynamical behavior of the LIV parameter and the best proposition for the time dependence of it should be searched for by studying quantum gravity in the early Universe. However, such a study is beyond the scope of the present work [3,4]. Substituting Eq. (21) into Eq. (9), the dispersion relation will take different forms within the two asymptotic regions in the early and late Universe. At the beginning of the time interval, $t\to-\infty$, the dispersion relation represents the form $\omega^2 = k^2 + m^2 - \sigma_0^2k^4$ and at the late time, $t\to+\infty$, it is converted to the standard form, i.e., Eq. (2). Now, using Eq. (21), we can obtain the general solution of Eq. (20) as follows:

$$\begin{aligned} T_k(t) = {} & C_1 e^{-i\tilde{\omega}_k t}F(a,b;c;-e^{\delta_0 t}) \\ & + C_2 e^{+i\tilde{\omega}_k t}F(b^* a^*; c^*; -e^{\delta_0 t}), \end{aligned} \tag{22}$$

where $F$ denotes the hypergeometric function, $\tilde{\omega}_k = \sqrt{k^2+m^2-\sigma_0^2k^4}$, and

$$\begin{aligned} a &= -i(\tilde{\omega}_k + \omega_k)/\delta_0, \\ b &= -i(\tilde{\omega}_k - \omega_k)/\delta_0, \\ c &= 1 - 2i\tilde{\omega}_k/\delta_0. \end{aligned} \tag{23}$$

To investigate the asymptotic behavior of the solution Eq. (22), we utilize Eq. (12), where $\tilde{u}_k(t,x) = e^{i\mathbf{k}.\mathbf{x}}\tilde{T}_k(t)$ and $u_k(t,x) = e^{i\mathbf{k}.\mathbf{x}}T_k(t)$. Thus, for the in region, $T\to-\infty$, and for the out region, $T\to+\infty$, the temporal factors of the solutions are obtained as

$$\tilde{T}_k(t) = \frac{1}{\sqrt{4\pi\tilde{\omega}_k}}e^{-i\tilde{\omega}_k t}F(a,b;c;-e^{\delta_0 t}), \tag{24}$$

$$\begin{aligned} T_k(t) = \frac{\sqrt{4\pi\omega_k}}{4\pi\tilde{\omega}_k}\Bigg( & e^{-i\tilde{\omega}_k t}\frac{\Gamma(c^*)\Gamma(a^*-b^*)}{\Gamma(a^*)\Gamma(c^*-b^*)}F(a,b;c;-e^{\delta_0 t}) \\ & + e^{+i\tilde{\omega}_k t}\frac{-\Gamma(c)\Gamma(b-c)}{\Gamma(b)\Gamma(c-a)}F(a,b;c;-e^{\delta_0 t})\Bigg), \end{aligned} \tag{25}$$

where $\Gamma(a)$ is the gamma function. The Bogoliubov coefficient values are obtained using the hypergeometric function properties as follows:

$$\alpha_k = \sqrt{\frac{\omega_k}{\tilde{\omega}_k}} \frac{\Gamma(c^*)\Gamma(a^* - b^*)}{\Gamma(a^*)\Gamma(c^* - b^*)}, \quad (26)$$

$$\beta_k = \sqrt{\frac{\omega_k}{\tilde{\omega}_k}} \frac{-\Gamma(c)\Gamma(b-c)}{\Gamma(b)\Gamma(c-a)}. \quad (27)$$

Using Eq. (15) together with Eq. (27), we can find the number of particle creation. According to the properties of the gamma function, the number of particle creation can be obtained as

$$\langle N_k \rangle = \frac{\sinh^2 [\pi(\omega_k - \tilde{\omega}_k)/\delta_0]}{\sinh(2\pi\tilde{\omega}_k/\delta_0)\sinh(2\pi\omega/\delta_0)}. \quad (28)$$

Therefore, the initial vacuum state is converted to an excited state in which the number of the particle is given by the above equation.

If the LIV occurs in a quantum adiabatic limit (i.e., there is no transition between different energy levels during the LIV), the particle creation, Eq. (28), is zero. An adiabatic scenario happens when either the coupling of the field and spacetime disappears through vanishing of the constant value of the LIV parameter, $\sigma_0$, or the rate of the LIV parameter evolution is quasistatic, $\delta_0 \to 0$. There is no difference between the initial and final vacuum in an adiabatic evolution (so that these states cannot be distinguished from each other), which leads to $\omega_k = \tilde{\omega}_k$. Therefore, the numerator of the fraction vanishes and the number of particle creation is zero, as expected.

## V. ENTANGLEMENT AND THERMODYNAMIC ENTROPY IN THE FLAT SPACETIME

In Sec. III, we saw that the creation and annihilation operators of "in" and "out" modes that were defined with respect to spatial mode decomposition are associated with the Bogoliubov transformation. As shown in Eq. (13), there is mixing only between the modes of frequency $k$ and $-k$. Thus, we concentrate on these modes and neglect the effects of other modes on the field. As a consequence, the vacuum state of the far past can be provided as a two-mode squeezing state and can be represented as a Schmidt decomposition as follows:

$$|\tilde{0}_k\tilde{0}_{-k}\rangle = \sum_n A_n |n_k\rangle|n_{-k}\rangle, \quad (29)$$

where $\{|n_k\rangle\}$ is the number of excitations in the mode of $k$. By applying the definition of vacuum state $a_k|0\rangle = 0$ along with Eq. (13) we deduce $A_n = (\frac{\beta_k^*}{\alpha_k^*})^n A_0$. From the normalization condition we find $|A_0|^2 = 1 - |\frac{\beta_k}{\alpha_k}|^2$. Therefore, the vacuum state for the in region is represented as

$$|\tilde{0}_k\rangle = \frac{1}{|\alpha_k|} \sum_{n=0}^{\infty} \left(\frac{\beta_k^*}{\alpha_k^*}\right)^n |n_k\rangle|n_{-k}\rangle. \quad (30)$$

To analyze the entanglement of the state given in the above equation, we employ the density matrix describing excitations in the modes of frequency $k$ and $-k$ as follows:

$$\rho_{k,-k} = |0_k 0_{-k}\rangle\langle 0_k 0_{-k}|. \quad (31)$$

The state in Eq. (30) is pure. Thus, the von Neumann entropy of the reduced density matrix is a suitable measure to identify entropy production between the modes $k$ and $-k$. We then get the von Neumann entropy as

$$S(\rho_k) = -\mathrm{Tr}[\rho_k \log \rho_k], \quad (32)$$

where $\rho_k = \underset{-k}{\mathrm{Tr}}[\rho_{k,-k}]$ is the reduced density matrix which can be obtained by tracing out the mode $-k$ in the state Eq. (30), as follows:

$$\rho_k = \frac{1}{|\alpha_k|^2} \sum_n \left(\frac{|\beta_k|}{|\alpha_k|}\right)^{2n} |n_k\rangle\langle n_k|. \quad (33)$$

By defining $\gamma \equiv |\frac{\beta_k}{\alpha_k}|^2$, it is clear that eigenvalues of the diagonal density matrix, Eq. (33), are $\lambda_n = (1-\gamma)\gamma^n$ and the von Neumann entropy is computed as

$$S_{\mathrm{en}} = S(\rho_k) = \log\left(\frac{\gamma^{\frac{\gamma}{\gamma-1}}}{1-\gamma}\right). \quad (34)$$

Recently, a quantum thermodynamic approach has been developed to investigate the entropy production in terms of the inner friction [73,77–79]. It has been established that the quantum fluctuations due to the field lead to inner friction, which can be considered as entropy interpretation. Here, we review the approach presented in [73] quickly, and then extend it to a LIV scenario. As a starting point, we suppose that the vacuum state of the initial Universe in the far past is unstable and can be viewed as a superposition of $|n_k n_{-k}\rangle$ in the far future. In fact, the LIV term has the role of fluctuations that changes the initial state to the final one. Similar to dynamical spacetime, we can argue that the LIV can do thermodynamical work. In a thermodynamical framework, we consider mode pairs of the field as a system and take the initial quantum gravity regime, emanating from the dominant gravitational field in the in region, as a work reservoir. From this viewpoint, the quantum gravity effects can be understood as a source to do work onto the quantum field and consequently move the quantum field away from the equilibrium state. We use a two-mode squeezing model to describe the thermodynamics of the current system. Therefore, any pairs of modes interact with each other and there is no interaction between the mode pairs and other modes of the field.

Based on the proposed discussion we can take advantage of the two-mode squeezing model. This procedure is in analogy with the quantum optical process [80–82]. We adopt the initial and final Hamiltonian as follows:

$$\tilde{H} = \tilde{\omega}_k(\tilde{a}_k{}^\dagger \tilde{a}_k + \tilde{a}^\dagger_{-k}\tilde{a}_{-k} + 1),$$
$$H = \omega_k(a^\dagger_k a_k + a^\dagger_{-k}a_{-k} + 1). \tag{35}$$

Since there is no interaction term in the Hamiltonian and the relation between creation and annihilation operators is given by Eq. (13), each pair of modes evolves unitarily, which is consistent with the above considerations. The average of works performed during the unitary evolution due to the LIV of the Hamiltonian from $\tilde{H}$ to $H$ is given by

$$W \equiv \mathrm{Tr}[H\rho_k] - \mathrm{Tr}[\tilde{H}\rho_k], \tag{36}$$

which indeed shows the average energy variation involved in the transfer process of $\tilde{H}$ to $H$. For an initial state defined in the vacuum state, Eq. (33), we have $\mathrm{Tr}[\tilde{H}\rho_k] = \tilde{\omega}_k$ and $\mathrm{Tr}[H\rho_k] = (\langle N_k\rangle + 1)\omega_k$. Thus, the average work is obtained as

$$\langle W\rangle = \omega_k\langle N_k\rangle + (\omega_k - \tilde{\omega}_k), \tag{37}$$

which implies energy changes in relation to particle creation and energy changes in a ground state. In a quantum adiabatic limit there are no transitions between energy levels, and particle creation does not occur. Therefore, the inner friction, defined as the difference between the total average work and the average of adiabatic work, only depends on the work related to particle creation,

$$\langle W\rangle_{\mathrm{friction}} = \omega_k\langle N_{\mathrm{k}}\rangle. \tag{38}$$

The entropy production fluctuation theorem [83–86] is used to demonstrate that the inner friction can be deduced as entropy production in the cosmological context [73], as follows:

$$\langle s\rangle = \frac{\langle W\rangle_{\mathrm{friction}}}{T} = \frac{\omega_k}{T}\langle N_{\mathrm{k}}\rangle. \tag{39}$$

To evaluate Eq. (39), we show that the reduced density matrix Eq. (33) can be rewritten as a thermal state. Let $z_k$ be the squeezing parameter; from Eq. (14) we can define the Bogoliubov coefficients as $|\alpha_k| \equiv \cosh z_k$ and $|\beta_k| \equiv \sinh z_k$. Substituting this into Eq. (33) yields

$$\rho_k = \frac{1}{\cosh^2 z_k}\sum_n \tanh^{2n} z_k |n_k\rangle\langle n_k|. \tag{40}$$

The above quantity corresponds to a thermal state as follows:

$$\rho_k = (1 - e^{-\frac{\omega_k}{T}})\sum_{n_k} e^{-\frac{\omega_k}{T}n_k}|n_k\rangle\langle n_k|, \tag{41}$$

where $\tanh z_k \equiv e^{-\frac{\omega_k}{T}}$, $\frac{\omega_k}{2}$ is associated with the ground state energy of the positive frequency modes as given by Eq. (30). Thus, the number of particle creation, $\langle N_k\rangle = \mathrm{Tr}(\rho_k N_k)$, appears as the Bose-Einstein distribution,

$$\langle N_k\rangle = (1 - e^{-\frac{\omega_k}{T}})\sum_{n_k} n_k e^{\frac{-\omega_k}{T}n_k} = \frac{1}{e^{\frac{\omega_k}{T}} - 1}. \tag{42}$$

The result provided in Eq. (42) implies a Planck spacetime at the temperature,

$$T = \frac{\omega_k}{2\log\frac{1}{\tanh z_k}} = \frac{\omega_k}{\log(\frac{1}{\gamma})}. \tag{43}$$

Consequently we have

$$T = \frac{\omega_k}{\log\left(1 + \mathrm{csch}[\frac{\pi}{\delta_0}(\omega_k - \tilde{\omega}_k)]^2 \sinh[\frac{\pi}{\delta_0}2\omega_k]\sinh[\frac{\pi}{\delta_0}2\tilde{\omega}]\right)}. \tag{44}$$

The behavior of temperature with respect to mass, $m$, and momentum mode, $k$, is shown in Fig. 1. The larger momentum modes correspond to higher temperatures. All momentum modes are involved to reach an adequately high temperature. Also, Fig. 2 implies that the temperature grows as the absolute value of the LIV parameters ($\sigma_0^2$ and $\delta_0$) increases.

Using Eq. (43), particle creation entropy will be evaluated as follows:

$$S_{\mathrm{cr}} = \langle s\rangle = \langle N_{\mathrm{k}}\rangle\log\left(\frac{1 + \langle N_{\mathrm{k}}\rangle}{\langle N_{\mathrm{k}}\rangle}\right). \tag{45}$$

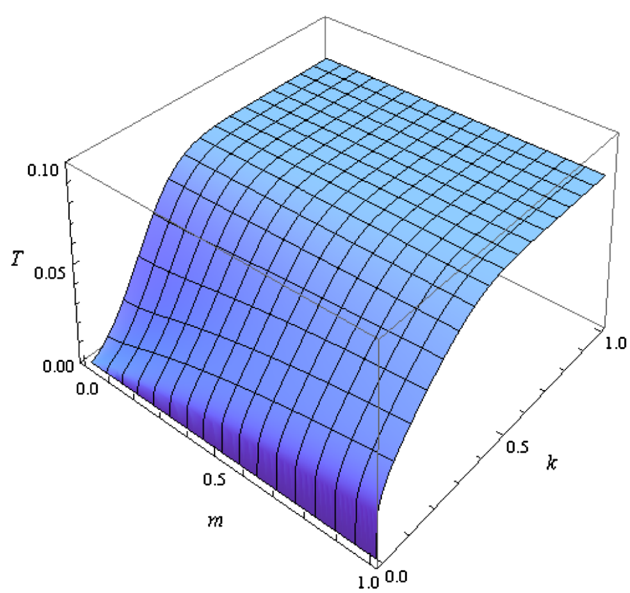


FIG. 1. Temperature as a function of momentum $k$ and mass $m$ for fixed values $\sigma_0^2 = -15, \delta_0 = 1$.

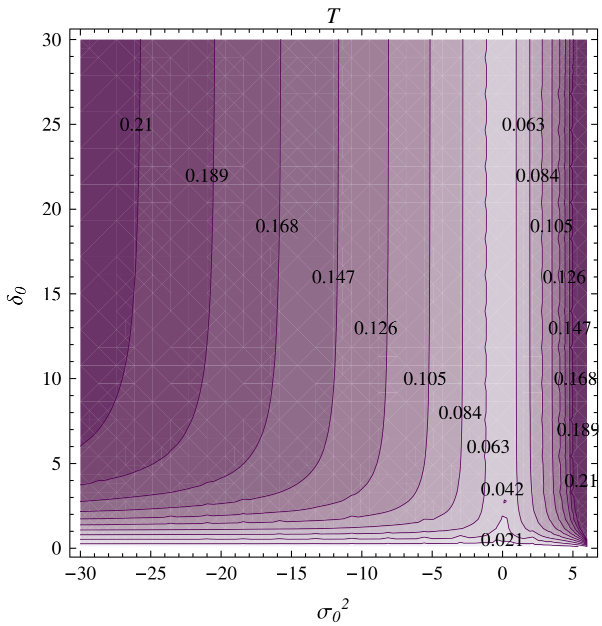


FIG. 2. Contour plot of the temperature with respect to the LIV parameters $\sigma_0^2$ and $\delta_0$ for the fixed values $m = 0$ and $k = 0.4$.

Here $\langle N_k \rangle$ is given by Eq. (15). The particle creation entropy can be rewritten as

$$S_{\mathrm{cr}} = \log(\gamma^{\frac{\gamma}{\gamma-1}}). \tag{46}$$

It seems that relation Eq. (46) shows a few similarities with the relation given in Eq. (34). The difference between both quantities is a factor $1-\gamma$ in the denominator of the logarithm function, which only appears in the entanglement entropy.

## VI. THE BEHAVIOR OF ENTANGLEMENT AND THERMODYNAMIC ENTROPIES IN FLAT SPACETIME

In this section we investigate the behavior of entanglement entropy obtained from quantum information theory. Moreover, we consider the thermodynamic entropy according to the quantum thermodynamic approach. The former is related to von Neumann entropy, while the latter comes from employing the approach to entropy production that stems from particle creation, as presented in Sec. VI. To compare and recognize the similarities of these two mentioned entropies, we have used the diagrammatic representations of two entropies with respect to field quantities, i.e., mass and the momentum of the modes, in Figs. 3 and 4.

As it is observed in Figs. 3 and 4, two quantities behave in the same way and the existence of the factor $1-\gamma$ in $S_{\mathrm{en}}$ only causes a slight increase in the value of entanglement entropy with respect to particle creation entropy. Entropy is known as a monotonic decreasing function of mass, and the

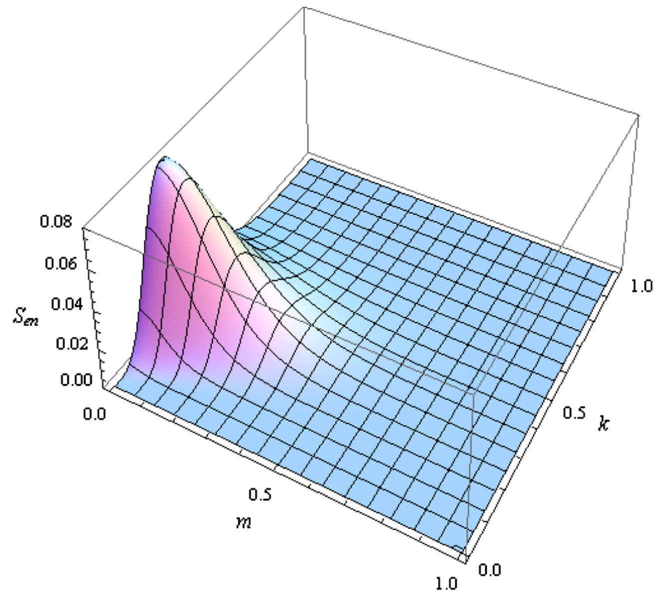


FIG. 3. Entanglement entropy as a function of momentum $k$ and mass $m$ for fixed values $\sigma_0^2 = -15, \delta_0 = 1$.

massless modes reveal the maximum value of entropy. This can be interpreted intuitively by the fact that modes with a smaller mass more easily emerge by evolution of the spacetime since the use of energy to supply the rest mass of modes with small mass is cheaper than high mass particles. Spectral behavior of entropies shows how entanglement or particle creation entropy depends on momentum of the field mode. Entropy with respect to momentum modes has maxima. There is a specific momentum for each mode, $k_{\mathrm{max}}$, so that entropy is maximum at this momentum mode. In fact, entropy peaks at a certain momentum, i.e.,

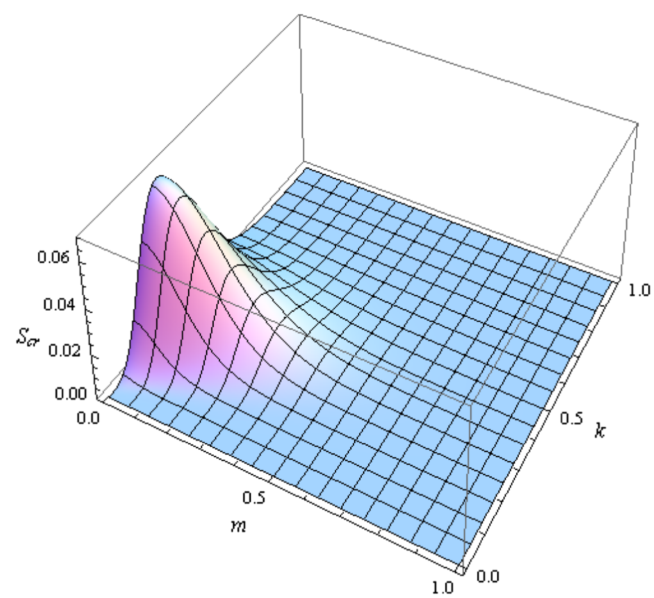


FIG. 4. Particle creation entropy as a function of momentum $k$ and mass $m$ for fixed values $\sigma_0^2 = -15, \delta_0 = 1$.

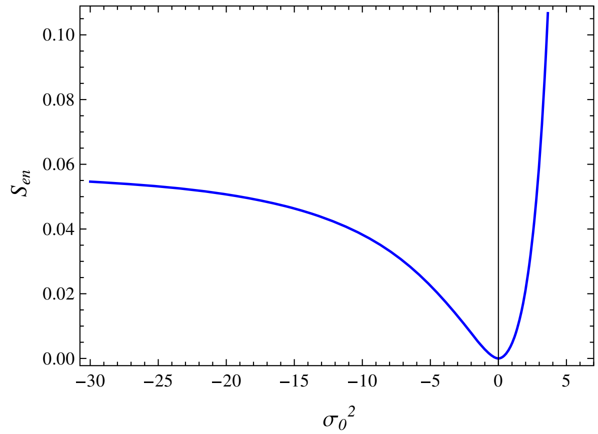


FIG. 5. Entanglement entropy, $S_{\mathrm{en}}$, as a function of the parameter $\sigma_0^2$, for the fixed values $m = 0$, $k = 0.4$, and $\delta_0 = 1$. Note that for the case $k = 0.4$, $\tilde{\omega}_k$ becomes imaginary for $\sigma_0^2 > 6.25$; thus the plot is not shown for this forbidden region.

the optimal value of $|k|$. Therefore, a large amount of entropy is generated for this privileged value of $|k|$. This means that modes of this characteristic frequency are far more prone to entanglement than any others. The optimal value of $|k|$ can be related to a characteristic wavelength that is increasingly correlated with a characteristic length of the Universe. There is no entropy for the zero momentum mode. This means that entanglement is zero, if the momentum mode of the field vanishes. This is the result of equivalence between in and out regions remaining invariant under time evolution, because the LIV term is absent. Thus, when the Lorentz invariance is violated, the field modes are in a state of entanglement. The other results as will be shown in the following are similar, so we will concentrate on the behavior of entanglement entropy independently.

Figure 5 shows the entanglement entropy as a function of $\sigma_0^2$. There are two distinct ranges for $\sigma_0^2$. The negative values are always valid to define $\tilde{\omega}_k$. However, for the positive one, there is an upper bound for $k$. The quantity $\tilde{\omega}_k$ will be imaginary for the value of $k$ greater than the upper bound. For the case shown in Fig. 5, i.e., $k = 0.4$, the region $\sigma_0^2 > 6.25$ is due to the forbidden region. As is seen, the entanglement entropy increases with respect to the absolute value of $\sigma_0^2$.

The entanglement entropy in terms of momentum mode $k$ for constant parameters $m = 0$ and $\delta_0 = 1$ is plotted in Fig. 6. Four different values of parameter $\sigma_0^2$ have been considered in this figure. The entropy decreases as the parameter $\sigma_0^2$ gets lesser values, regardless of a negative sign. The spacetime structure selects one value of the momentum mode for which the time evolution of LIV produces a larger amount of entanglement. This selection is sensitive to the LIV parameter $|\sigma_0^2|$. As $|\sigma_0^2|$ is increased, the plot is rescaled. Except for $\sigma_0^2 = 1$ that exhibits no value for

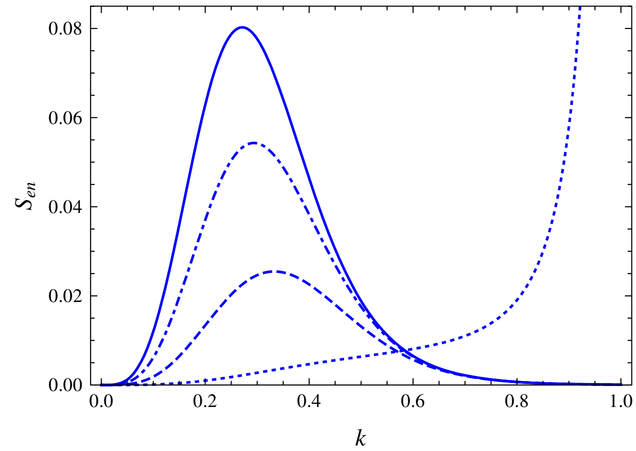


FIG. 6. Entanglement entropy $S_{\mathrm{en}}$, as a function of momentum mode $k$ for the fixed values $m = 0$, $\delta_0 = 1$, and four different values of parameter $\sigma_0^2$, i.e., $\sigma_0^2 = -15$ (solid line), $\sigma_0^2 = -10$ (dotted-dashed line), $\sigma_0^2 = -5$ (dashed line), and $\sigma_0^2 = 1$ (dotted line). Note that for the case $\sigma_0^2 = 1$, $\tilde{\omega}_k$ becomes imaginary for $k > 1$; thus the plot is not shown for this forbidden region.

$k_{\mathrm{max}}$, for other cases, $k_{\mathrm{max}}$ is shifted to more positive values with decreasing parameter $\sigma_0^2$. Therefore, for smaller LIVs, a larger frequency mode is more entangled.

A synchronous analysis of the LIV parameter requires representation of the entanglement entropy in terms of $\sigma_0^2$ and $\delta_0$ as shown in Fig. 7. As can be seen, the entanglement entropy increases by any increment in the absolute value of $\sigma_0^2$ and $\delta_0$. Also, for a large enough value of $\delta_0$, it is possible to specify entanglement entropy as a constant function of $\delta_0$. It is important to note that entanglement is very sensitive

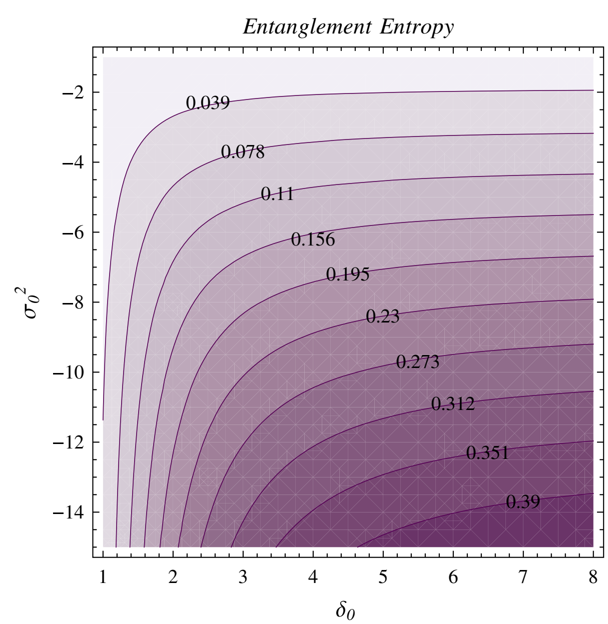


FIG. 7. Contour plot of the entanglement entropy with respect to the LIV parameters $\sigma_0^2$ and $\delta_0$ for the fixed values $m = 0$ and $k = 0.4$.

with respect to $|\sigma_0^2|$ but becomes insensitive to variations within the parameter $|\delta_0|$, when $|\delta_0|$ is increased. The level curves of entanglement entropy show a rapid increase as $|\delta_0|$ grows and thus a larger entanglement is generated, However, there is a saturation level, for large enough values of $|\delta_0|$.

## VII. ON THE CURVED SPACETIME

In this section we deal with studying the effects of LIV on the behavior of particle creation and entanglement entropies in a curved spacetime. To this aim let us begin with a $(1+1)$-dimensional FRW background metric. However, in such a spacetime, a global Killing vector field could not be found and thus will not be able to find separable solutions to the wave equation in order to classify the modes. However, there may exist two asymptotically flat regions in the past and future times. Therefore, we can introduce a timelike Killing vector and find a complete basis based on a set of positive and negative frequency solutions to the Klein-Gordon equation. Then, the field is expanded in terms of the modes by interpreting creation and annihilation operators as coefficients of the extension. Therefore, the particle number is well defined. The line element of the FRW spacetime can be parametrized as

$$ds^2 = dt^2 - a^2(t)dx^2, \tag{47}$$

where $a(t)$ is the scale factor. By defining the conformal time as $d\eta = a^{-1}dt$, the above metric will take the form

$$ds^2 = \Omega^2(\eta)(d\eta^2 - dx^2), \tag{48}$$

where $\Omega^2(\eta)$ is the conformal scale factor. The generalized Lagrangian for the spacetime described above is given by

$$\mathcal{L} = \frac{1}{2}\sqrt{-g}[g^{\mu\nu}\nabla_\mu\phi\nabla_\mu\phi - m^2\phi^2 + \sigma^2(D^2\phi)^2 + \lambda(1 - u^\mu u_\mu)], \tag{49}$$

where $g^{\mu\nu}$ corresponds to Eq. (47). The covariant form of the spatial Laplacian, Eq. (17), is given by

$$D^2\phi = -D^\mu D_\mu\phi = -q^{\mu\nu}\nabla_\nu(q_\mu^\tau\nabla_\tau\phi),$$

where

$$q_{\mu\nu} = -\eta_{\mu\nu} + u_\mu u_\nu, \qquad \eta^{\mu\nu}u_\mu u_\nu = 1.$$

The $\lambda$ coefficient in the last term of the Lagrangian, Eq. (49), constrains $u^\mu$ as

$$g_{\mu\nu}u^\mu u^\nu = 1.$$

Since the FRW metric describes a homogeneous and isotropic spacetime, $u_\mu$ should admit these properties. The four-vector velocity can then be obtained as $u^\mu \equiv (\Omega(\eta), 0)$ whence the equation governing the evolution of the scalar field reads

$$\left[\Box - \Omega^2(\eta)m^2 - \frac{\sigma^2}{\Omega^2(\eta)}\partial_x^4\right]\phi = 0, \tag{50}$$

where the d'Alembertian operator is $\Box\phi \coloneqq g^{\mu\nu}\nabla_\mu\nabla_\nu\phi = \frac{1}{\sqrt{-g}}\partial_\mu(\sqrt{-g}g^{\mu\nu}\partial_\nu\phi)$. Now, we pick out the conformal scale factor as follows:

$$\Omega^2(\eta) = 1 + \epsilon(1 + \tanh(\rho\eta)), \tag{51}$$

where $\epsilon$ is the expansion volume and $\rho$ indicates the expansion rate. We prefer Eq. (51) over other choices, since for $\eta \to -\infty$, the metric takes the form

$$ds^2 = (d\eta^2 - dx^2),$$

and for $\eta \to +\infty$ the metric reads

$$ds^2 = (1 + 2\epsilon)(d\eta^2 - dx^2).$$

Consequently, the spacetime is asymptotically flat and admits Killing symmetries in these regions. We can use the method of separation of variables to select solutions to Eq. (50) as $u_k(\eta, x) = e^{ikx}\chi_k(\eta)$. Thus, Eq. (50) is reduced to

$$\left[\partial_\eta^2 + k^2 + \Omega^2(\eta)m^2 - \frac{\sigma^2}{\Omega^2(\eta)}k^4\right]\chi_k(\eta) = 0. \tag{52}$$

To find the exactly solvable solutions, we suppose the massless case, $m = 0$, without loss of generality. Therefore, in the far past region, i.e., the in region where $\eta \to -\infty$, we have

$$\begin{aligned}\tilde{\chi}_k(\eta) = &\frac{1}{\sqrt{4\pi\tilde{\omega}_k}} \\ &\times \exp\left(-i\omega_k^+\eta - i\frac{\omega_k^-}{\rho}\ln\left[(1+2\epsilon)e^{\rho\eta} + e^{-\rho\eta}\right]\right) \\ &\times F(1 + i\omega_k^-/\rho, i\omega_k^-/\rho; 1 - i\tilde{\omega}_k/\rho; z),\end{aligned} \tag{53}$$

$$\begin{aligned}\chi_k(\eta) = &\frac{1}{\sqrt{4\pi\tilde{\omega}_k}} \\ &\times \exp\left(-i\omega_k^+\eta - i\frac{\omega_k^-}{\rho}\ln\left[(1+2\epsilon)e^{\rho\eta} + e^{-\rho\eta}\right]\right) \\ &\times F(1 + i\omega_k^-/\rho, i\omega_k^-/\rho; 1 - i\omega_k/\rho; z),\end{aligned} \tag{54}$$

where $F(a, b; c; z)$ denotes the hypergeometric function and

$$\tilde{\omega}_k = \sqrt{k^2 - \sigma^2 k^4}$$
$$\omega_k = \sqrt{k^2 - \frac{\sigma^2}{1+2\epsilon} k^4}$$
$$\omega_k^{\pm} = \frac{1}{2}(\omega_k \pm \tilde{\omega}_k)$$
$$z = \frac{1+2\epsilon}{2} \frac{1+\tanh(\rho\eta)}{1+\epsilon\tanh(\rho\eta)}. \tag{55}$$

The performance of field quantization in curved spacetime is similar to Minkowskian spacetime. According to Eq. (12) together with the linear transformation properties of hypergeometric functions, the Bogoliubov coefficients are evaluated as

$$\alpha_k = \sqrt{\frac{\omega_k}{\tilde{\omega}_k}} \frac{\Gamma(1 - i\tilde{\omega}_k/\rho)\Gamma(-i\omega_k/\rho)}{\Gamma(-i\omega_k^+/\rho)\Gamma(1 - i\omega_k^+/\rho)}, \tag{56}$$

$$\beta_k = \sqrt{\frac{\omega_k}{\tilde{\omega}_k}} \frac{\Gamma(1 - i\tilde{\omega}_k/\rho)\Gamma(i\omega_k/\rho)}{\Gamma(i\omega_k^-/\rho)\Gamma(1 + i\omega_k^-/\rho)}. \tag{57}$$

Therefore, the number of particle creations per mode $k$ is given by

$$\langle N_k \rangle = \frac{\sinh^2(\pi\omega_k^-/\rho)}{\sinh(\pi\tilde{\omega}_k/\rho)\sinh(\pi\omega_k/\rho)}, \tag{58}$$

The above result is obtained by a simple calculation from Equation (15) and (57). The properties of the gamma function have been used to deduce Equation (58).

To evaluate particle creation entropy according to the approach introduced in Sec. VI, we consider the thermodynamics framework so that the mode pair of the field is assumed as a system and the spacetime that acts on the quantum field as a work reservoir. The spacetime, including the effects of the initial quantum gravity regime (due to the dominant gravitational field), along with the evolution of spacetime owing to the expansion of the Universe as a source, does work on the quantum field and takes it away from equilibrium. Therefore, by following the process presented in Sec. VI, the temperature of Planck spacetime, Eq. (43), can be obtained as

$$T = \frac{\omega_k}{\log\left(1 + \mathrm{csch}[\frac{\pi\omega_k^-}{\rho}]^2 \sinh[\frac{\pi\tilde{\omega}_k}{\rho}] \sinh[\frac{\pi\omega_k}{\rho}]\right)}. \tag{59}$$

The temperature of the created particle spectrum with respect to momentum modes is illustrated in Fig. 8. The larger momentum modes lead to an increase in temperature and a high enough temperature produces all momentum modes. By increasing the expansion rate, a higher bound for the temperature is necessary for the production of modes. Figure 9 shows an upper temperature for a high enough LIV parameter, $\sigma^2$, and when the expansion volume, $\epsilon$, is close to the maximum value.

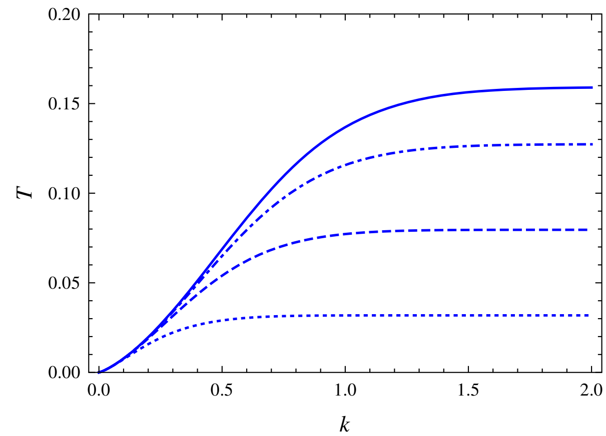


FIG. 8. Temperature as a function of the momentum modes, $k$, for fixed values $\epsilon = 0.99$ and $\sigma^2 = -1$, and for four different values of $\rho$, i.e., $\rho = 1$ (solid line), $\rho = 0.8$ (dotted-dashed line), $\rho = 0.5$ (dashed line), and $\rho = 0.2$ (dotted line).

The entanglement behavior is investigated by von Neumann entropy, Eq. (34), where $\gamma$ is obtained by using Eqs. (56) and (57). Figure 10 shows the entanglement entropy with respect to the momentum modes, $k$, and the expansion rate, $\rho$. As the expansion rate grows, the entanglement entropy increases accordingly. Therefore, the entanglement entropy is an increasing function of the expansion rate. In the curved spacetime in analogy with flat spacetime (as we saw in Sec. VI) the entanglement entropy represents a specific momentum mode, $k_{\max}$, for each mode. This specific momentum can maximize the entanglement entropy. A similar pattern of behavior is observed for thermodynamic entropy, Eq. (46), shown in Fig. 11. The other results obtained from the entanglement

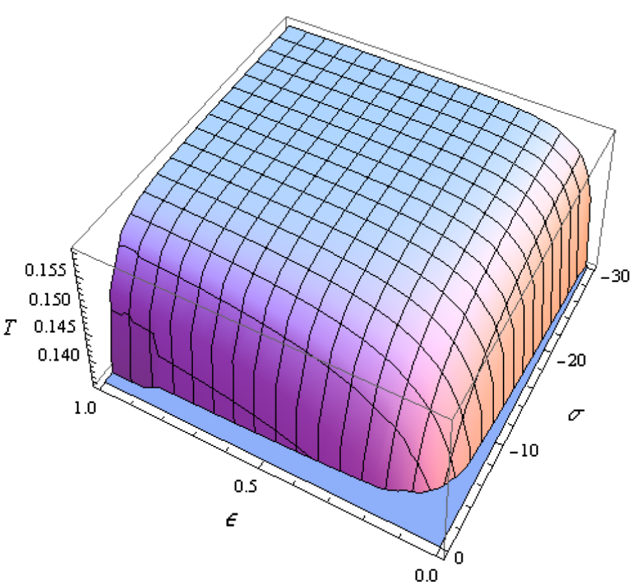


FIG. 9. Temperature in terms of the LIV parameter, $\sigma^2$, and the expansion volume, $\epsilon$, for the fixed values $k = 1$ and $\rho = 1$.

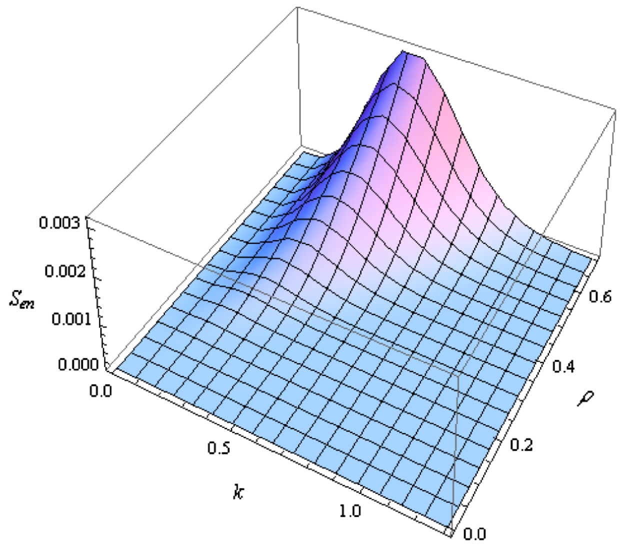


FIG. 10. Entanglement entropy in terms of the momentum, $k$, and the expansion rate, $\rho$, for the fixed values $\epsilon = 0.99$ and $\sigma^2 = -1$.

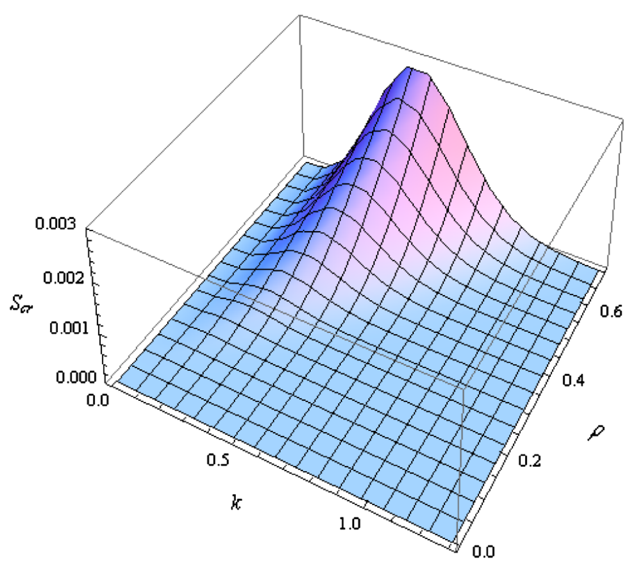


FIG. 11. Particle creation entropy in terms of the momentum, $k$, and the expansion rate, $\rho$, for the fixed values $\epsilon = 0.99$ and $\sigma^2 = -1$.

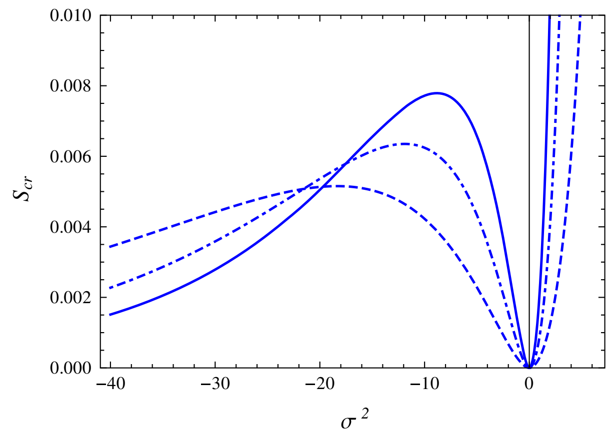


FIG. 12. Particle creation entropy, $S_{cr}$, as a function of the LIV parameter, $\sigma^2$, for fixed value $\epsilon = 0.99$ and three different values of $k$ and $\rho$, i.e., $k_{\max}$ with $\rho = 0.5$ (solid line), $\rho = 0.4$ (dotted-dashed line), and $\rho = 0.3$ (dashed line). Note that the plot is not shown for some regions where $\tilde{\omega}_k$ becomes imaginary.

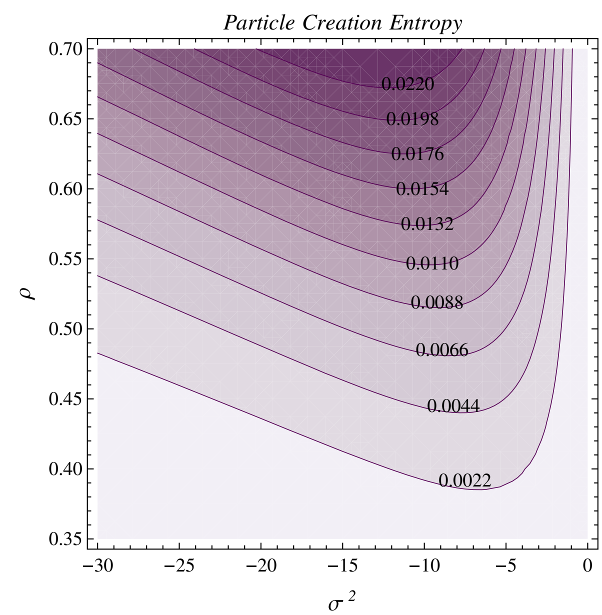


FIG. 13. Contour plot of the particle creation entropy with respect to the LIV parameter $\sigma^2$ and the expansion rate $\rho$ for the fixed values $\epsilon = 0.99$ and $k_{\max} = 0.4$.

and the particle creation entropies, as we illustrate in the following, are also similar. This time we will concentrate on the behavior of particle creation entropy independently.

Figure 12 shows the entanglement entropy in terms of the LIV parameter, $\sigma^2$. The plot is only shown for regions of $\sigma^2$ where $\tilde{\omega}_k$ is valid. For the valid positive values of $\sigma^2$, the particle creation entropy is an increasing function of $\sigma^2$. However, for negative values, which are always valid, the particle creation entropy increases for a while for a specific range of absolute values of $\sigma^2$ and then starts to decrease. In fact, particle creation entropy exhibits maxima which occur at a certain value of the LIV parameter, $\sigma^2_{\max}$. For each special expansion volume, $\sigma^2_{\max}$ is shifted toward negative values with decreasing expansion rate. As shown in Fig. 13. A decreasing expansion rate also leads to a decline in the value of particle creation entropy for $\sigma^2_{\max}$. Figure 14 shows the dependency of entropy on the volume expansion and the variation of entropy with respect to variations of the expansion rate. The particle creation entropy is an increasing function of expansion volume and grows as the expansion rate gets larger values. From this figure we can deduce that the entropy for reliable positive values of $\sigma^2$

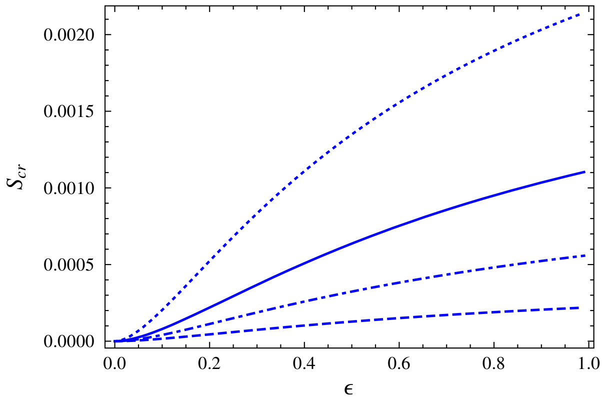


FIG. 14. Particle creation entropy $S_{\mathrm{cr}}$, as a function of expansion volume $\epsilon$, for fixed value $\sigma^2 = -1$ and three different values of $k$ and $\rho$, i.e., $k_{\mathrm{max}}$ with $\rho = 0.5$ (solid line), $\rho = 0.4$ (dotted-dashed line), and $\rho = 0.3$ (dashed line), and also for the fixed values $\sigma^2 = 1$, $k_{\mathrm{max}}$, and $\rho = 0.5$ (dotted line).

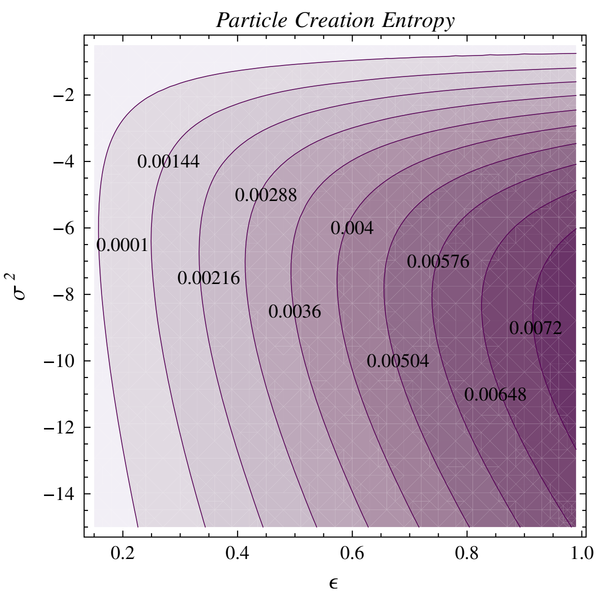


FIG. 15. Contour plot of the particle creation entropy with respect to the LIV parameter $\sigma^2$ and the expansion volume $\epsilon$ for the fixed values $p = 0.5$ and $k_{\mathrm{max}} = 0.4$.

grows more than the entropy for the same negative values of $\sigma^2$. The contour plot of the particle creation entropy with respect to the LIV parameter $\sigma^2$ and the expansion volume $\epsilon$ is shown in Fig. 15. It is obvious that the entropy increases by increasing the value of $\epsilon$. Also, for a fixed value of $\epsilon$ we can fix a maximum entropy for a special value of $\sigma^2$.

## VIII. THE DEPENDENCE OF ENTROPY ON COSMOLOGICAL PARAMETERS

In both flat and curved spacetimes, the amount of entropy generated in the field due to LIV codifies information about the underlying spacetime, although, as the

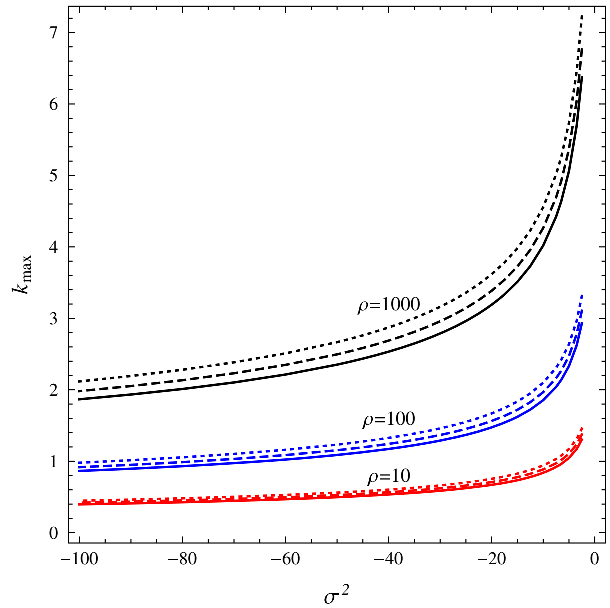


FIG. 16. Optimal $|k|$ (mode with maximum entropy) as a function of the LIV parameter $\sigma^2$ for different values of $\epsilon = 0.2, 0.5, 0.99$ (solid, dashed, dotted) and $\rho = 10, 100, 1000$.

momentum of the field varies, the behavior of entropy seems similar as is shown in Figs. 3, 4, 10, and 11. However, there are differences between flat and curved models, in the amount of information that the two states of entropy could provide with respect to the LIV parameter. Having this in mind, we can control the expansion volume of the Universe in a curved model and investigate the behavior of entropy with respect to the LIV parameter for different values of this parameter. Figure 5 shows how the entropy depends on the LIV parameter in the flat model when the Universe evolves from early time to late time, where the LIV term in Eq. (20) entirely vanishes. The curved model represents similar behavior when the total volume of the Universe is close to a very large value. But in the case in which we deal with curved spacetimes where the total volume of the Universe is still small, Fig. 12, the entropy reaches a maximum value at a certain LIV parameter, while for a very large volume value, entropy increases monotonically with $|\sigma^2|$. In contrast to the flat case and also the curved case where the volume value is very large, in the curved case where the volume value is small, there is a privileged value of $|\sigma^2|$ for which the expansion of spacetime generates a large amount of entropy. This natural emergence of a privileged LIV parameter in curved spacetime is very sensitive to expansion parameters and is thus more efficient (in comparison to the flat case) for encoding information about the underlying spacetime. We benefit from this special behavior for curved spacetime and also from the characteristic peak that the entropy presents at a certain momentum to design a method to extract information on cosmological parameters.

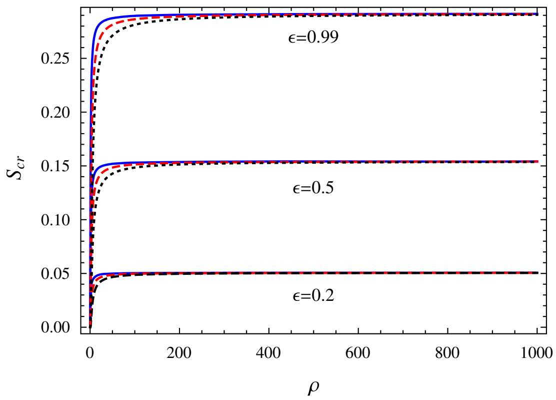


(a)

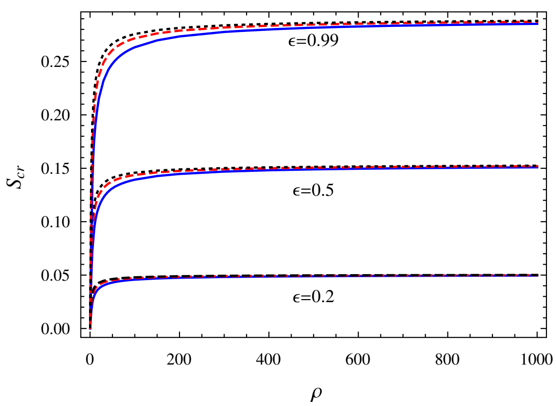


(b)

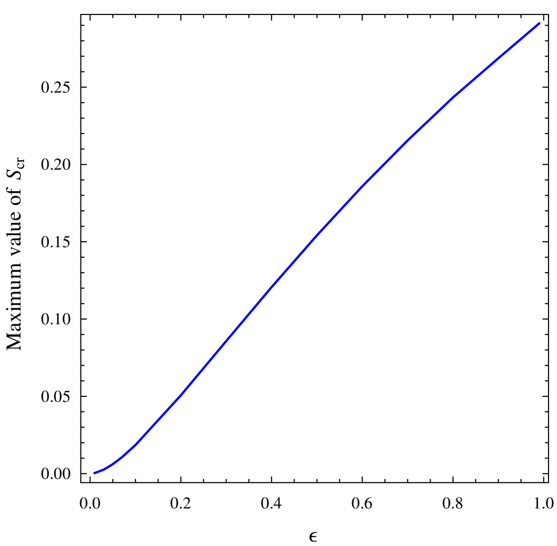


(c)

FIG. 17. (a) $S_{cr}$ in the line of optimal $|\sigma^2|$ as a function of $\rho$ for different values of $\epsilon = 0.2$, 0.5, 0.99 and the LIV parameter $\sigma^2 = -5, -15, -30$ (solid, dashed, dotted). (b) $S_{cr}$ in the line of optimal $|k|$ as a function of $\rho$ for different values of $\epsilon = 0.2$, 0.5, 0.99 and mode $k = 0.2$, 0.5, 1 (solid, dashed, dotted). (c) Maximum entropy achievable (optimal $|k|$ and $|\sigma^2|$) as a function of $\epsilon$. It does not depend on $\rho$.

In Fig. 16, we present the frequency at which the maximum value for the entropy occurs, i.e., the optimal value of $|k|$. This value is extremely sensitive to the rapidity of the expansion of the Universe, while at the same time it has low sensitivity to variations with respect to the total volume of the Universe at the interval in which 0.99 of the total expansion occurs [30]. Therefore, without any need to assume a fixed $\epsilon$, we can take advantage of the optimal $|k|$ curve to estimate rapidity, independently of the volume.

Figure 17 shows that for different values of $\rho$ and $\epsilon$ the maximum value of the entropy at the optimal point of $|\sigma^2|$ is almost sensitive to only $\epsilon$ and insensitive to rapidity variations. Hence, information about $\epsilon$ as the geometric factor of the metric, which plays a geometric role, is encoded within the maximum achievable entropy at the optimal value of $|\sigma^2|$. Also, the amount of entropy at the optimal mode $|k|$ of the field depends only on the total volume of expansion and there is no need to account for the rapidity variations as is represented in Fig. 17. Thus, information about volume is encoded in this peak. For a fixed value of $\epsilon$ and for different values of $\rho$, there is a maximum value of entropy at the optimal point such that the measured entropy is never larger than it. Figure 17 demonstrates how the maximum entropy achievable for the optimal frequency LIV parameter varies with the volume parameter $\epsilon$. Indeed, it does not depend almost on $\rho$. As a result, the information about $\epsilon$ is codified in maximum entropy. This presents a method to obtain a lower bound for the total volume regardless of the rapidity of the expansion.

We therefore conclude that the peak behavior of the entropy presents information about all the expansion parameters. Also, the optimal mode and LIV parameters can be related to each other via this peak. If we were able to search the field and detect the most entangled mode, this would provide us with a great deal of information about the characteristics of the spacetime background for a fixed expansion model.

## IX. DISCUSSION AND CONCLUSION

In the model herein, we considered a free scalar field on a spatial lattice. The effects of quantum gravity modify the standard dispersion relation to include an extra term and enforce the violation of Lorentz symmetry. Adding such a term is equivalent to including a vector field, coupled with a matter field, within the Lagrangian. Hence, the conformal invariance is broken and the particles are created such that the particle creation can be related to the current entropy content of the Universe. We followed two approaches in both flat and curved spacetimes, which render a connection between measures of entropy and amounts of particle creation in cosmological scenarios, i.e., von Neumann entropy and particle creation entropy. The von Neumann entropy characterizes the mixedness of a state, or in other words, if the state is observed as part of a pure entangled state, then it is the amount of entanglement in the total state. The particle creation entropy relates the phenomenon of particle creation to a thermodynamic quantity called inner friction, due to the quantum fluctuations of the fields. From this viewpoint, the quantum gravitational regime leads to enormous entropy production within the content of the Universe. This perhaps is due to the fact that the current entropy source of the Universe can be generated by the quantum structure of the geometry.

In the beginning, we focused our attention on flat spacetime and used past and future procedures to obtain two sets of exact solutions, which are connected via Bogoliubov transformation coefficients. The definition of the basis for early and late time is different since the dispersion relations for these two regions are not equal. By choosing a time-dependent LIV parameter, a geometric effect takes a separable pure state in early time to an entangled state at late time. We employed von Neumann entropy to analyze entropy increasing due to entanglement. Also, we evaluated the thermodynamic entropy, given by the fluctuation theorem. In this sense, the quantum structure of the geometry takes the field away from equilibrium and the inner friction work increases the entropy. Likewise, we explored the variation of two entropies with respect to the LIV and field parameters.

In curved spacetime, we followed the same steps as in our analysis in flat spacetime and studied von Neumann entropy and particle creation entropy in asymptotically flat Friedmann-Robertson-Walker spacetime. The dependence of these entropies on the LIV parameter, field parameters, and cosmic parameters can present information about the underlying structure of the spacetime. It is important to note that our results are general and can be applied to any scenario where Bogoliubov transformations are present in the dynamics of quantum fields.

What do we learn from these results? While previous works in scenarios without LIV have shown that the Dirac fields codify more information about the underlying expansion than the scalar fields [55], by relying on the scalar fields we can take advantage of expansion-generated entropy due to LIV. This helps us to obtain information about the underlying spacetime.

The expansion of the Universe generates entanglement for both scalar and Dirac field modes when the conformal symmetry is broken [55]. For the scalar case, a monotonically decreasing entanglement is observed as momentum increases and its maximum occurs at $|k| = 0$, while for the Dirac case, entanglement is maximized at a certain momentum, associated with a characteristic wavelength proportional to $|k|^{-1}$. The exclusion principle impedes the excitation of the fermionic modes whose $|k| \to 0$ (very long-wavelength modes) from being entangled by the underlying structure of the spacetime. However, this constraint does not exist for bosons. Thus, the entanglement is higher when $|k| \to 0$. What about large $|k|$ modes? Modes with large values for the $|k|$ parameter are more difficultly excited as the spacetime expands because these modes require much energy to be excited. Let us concentrate on a conformally invariant setting, for which expansion produces no entanglement between the field modes and thus no particle creation occurs.

For the massless case which we argued in Sec. VII, the theory is conformally invariant without the LIV term; thus, there is no more generated entanglement only due to expansion. By adding the LIV term to the field equation, the conformal invariance is broken and entropy is generated.

To interpret the observed results in this work we explain the entropy behavior in terms of the discreteness of the spacetime. For the sake of simplicity we have considered only the discretized one-dimensional space whose lattice parameter is the LIV length. The generalization to higher spatial dimensions and inclusion of the time discreteness is straightforward. In one dimension there is a single lattice parameter, i.e., the LIV parameter and one-dimensional reciprocal lattice. At the large spatial scales (large wavelengths), i.e., $|k| \to 0$, the dispersion of particles is close to the center of the Brillouin zone [87]. These solutions are just like the free particles with renormalized mass. It is understandable that for such very large wavelengths, the quantum length scale is less important. These wavelengths are close to the classical length scale and do not observe the effects of the LIV on the classical length scales. As is evident in our analysis, the calculated entropy for the scales larger than the quantum LIV length is meaningless and should tend to zero for the corresponding (small) momentum modes. It is interestingly fitted to the fermionic behavior which is known to vanish in this limit. Nevertheless, it is worth mentioning that the nature of the behavior is not the same for an expansion-generated fermionic field, as this behavior may be a consequence of the Pauli exclusion principle; but for our case, it is due to the fact that there is no entropy contribution for the scales larger than the quantum LIV length.

On the other hand, at small spatial scales (small wavelengths), i.e., $|k| \to \infty$, the system approaches to its continuous limit where the effects of discreteness are not felt by the particles (bosons in our case). Noting that the entropy considered in this paper is purely due to the effects of discreteness of the spacetime, then we expect that in the continuous limit ($|k| \to \infty$) the entropy tends to zero as is seen in our analysis. This behavior is common between Lorentz-invariant entanglement of fermions and bosons and the Lorentz-violated bosons considered in this paper. But again, we emphasize that the nature of this behavior is not the same; i.e., in the Lorentz-invariant models the entropy tends to zero for $|k| \to \infty$, since the excitation of the particles for the large momentum modes and therefore large energies can rarely occur. However, for our case (Lorentz-violated bosons) such behavior is due to the fact that the properties of the system are like the continuous model and the effects of the lattice parameter are not seen.

Therefore, we expect two asymptotic behaviors as the particle creation entropy tends to zero. These two asymptotic behaviors for entropy are related to modes whose $|k|$ is close to zero and infinity. This generally introduces a characteristic length scale in the problem under which the entropy should fall off rapidly. In other words, there should be a characteristic value for the wave number, namely, $k_{\mathrm{char}} \sim \sigma^{-1}$, at which a change in the behavior of entropy (increasing behavior to a decreasing behavior) can be observed. This behavior is seen in Fig. 12. The characteristic length is exactly fitted to the inverse of the edge vectors (boundaries) of the Brillouin zone, i.e., $k_{\mathrm{char}} \sim \sigma^{-1}$. Sets of the location $(k, \sigma)$ of maximal entropy fulfill the condition $k_{\mathrm{max}} \sim \sigma_{\mathrm{max}}^{-1}$.

Today, the researchers vastly try to make a connection between the phenomenon of entanglement and cosmology. Previous studies have analyzed the possibility of swapping this entanglement to local detectors [33,88–92]. Through the extraction of cosmological parameters from entanglement in field modes, we can compare our theoretical model with observational data. We analyzed the properties of produced entanglement (and generated entropy) of a quantum scalar field (minimally coupled to gravity), due to LIV directly, via the field itself. Using both a minimally and conformally coupled field, our model can also be considered in order to investigate the effects of LIV on the response of local detectors, hence providing a stronger grounding in operationalism [90]. It is worth emphasizing that although we rely on the scalar field, generated entropy due to LIV for the Dirac field would also be interesting.

The results of this paper can be generalized to conceive a better understanding of the process by which early Universe fluctuations in a scalar field are frozen into eventual classical density fluctuations within the matter distribution of the late Universe (and finally are led to temperature variations in cosmic microwave background (CMB)). The recent results about the effects of expansion on local detectors indicate that the entanglement vanishes at the Hubble horizon distance [91]. Moreover, Bose-Einstein condensates can give an experimental study of the freezing of quantum fluctuations into a classical density distribution beyond the sonic horizon [93].

One of the best candidates which provide information about our cosmology is CMB, based on the temperature maps produced by WMAP [94]. In the work herein, we showed that LIV in an expanding spacetime generates entanglement between certain modes of a gravitationally interacting scalar field. We will show elsewhere in detail how our model can be applied to other spacetimes that are more realistic. It is not, however, far-fetched to imagine that the entanglement within the scalar field modes which is responsible for the density fluctuations in the early Universe has been somehow transferred to other fields to which we have access today. In this sense, we might observe entanglement within the individual particles of CMB in the form of measurable temperature fluctuations such as the parametric down-conversion experiments [95,96] that have been carried out in order to verify the phenomenon of entanglement.

It is worth emphasizing individually that field modes entangled due to the gravitational interactions only when can be remained coherence that the fields are rarely interacting. The cosmic neutrino background may be a natural candidate for residual quantum correlations, since they are approximately only gravitationally interacting particles [97–100]. It is possible that entanglement of the cosmic neutrino background which weakly interacts with anything at all survives all the way to the present time and hence is detectable today. Therefore, the idea of searching for the neutrino background in order to use its degree of entanglement can involve information concerning our cosmic history and LIV in the early Universe. Despite the electromagnetic field, the neutrino background is not directly observable since these low energy particles rarely interact with the rest of the quantum fields. However, if we consider the improvement of the CMB spectrum as our sole criteria to analyze primordial cosmic entanglement, we should not dismiss the possibility of taking advantage of it as a reasonable candidate. On the other hand, due to the fact that the effects discussed above are difficult to test directly, there exist several simulations that provide the laboratory accessible testable data for cosmological models [93,101–109]. In such laboratory setups, the parameters of the experiment may be adjustable to provide much stronger and more easily observed effects, which are conceptually the same as the predictions of quantum fields on a curved spacetime.

Finally, as we approach the end of this paper, a few points beg further elucidation. The possibility of exploring the physics of quantum gravity with astrophysical observations and putting bounds on the generic quantum gravity effects and the parameters involved within the theory has been a great and challenging task during recent years [110]. New bounds [111] on isotropic LIV have been estimated in the pure photonic and gluonic sector of the standard model extension [113]. Therefore, to consider experimental bounds on the LIV parameters and the corresponding entropies, we need to take into account the dependence of these terms on polarization. The effective field theory can be adopted as a useful tool. A complete investigation of these issues would be interesting but lies beyond the scope of the present work. It is necessary to assess anisotropic models because of the anisotropy observed in the spectrum of the CMB [114,115]. The experimental bounds can become weaker if the assumption of isotropy is removed in the CMB frame [116]. In this paper, attention was given to isotropic FRW spacetime. Recently, the influence of anisotropy on entanglement produced by dynamical spacetime was studied using a Bianchi type I model [117]. In an upcoming work we plan to return to the issue raised by this paper with a detailed discussion of such a situation and to address the extent to which the generated entropy can be affected by an anisotropic model when the LIV is taken into account.

## ACKNOWLEDGMENTS

The authors would like to thank M. M. Sheikh-Jabbari, A. Naseh, and three anonymous referees for a careful reading of the manuscript and their helpful comments. The authors also appreciate N. Khosravi and M. N. Najafi for related discussions. M. F. extends special thanks to A. H. Ziaie for his comments and encouragement.

[1] M. B. Green, J. H. Schwarz, and E. Witten, *Superstring Theory* (Cambridge University Press, Cambridge, England, 1988), Vol. 1.
[2] J. Polchinski, *String Theory* (Cambridge University Press, New York, 1998), Vol. 1.
[3] C. Rovelli, *Quantum Gravity* (Cambridge University Press, New York, 2004).
[4] T. Thiemann, *Modern Canonical Quantum General Relativity* (Cambridge University Press, New York, 2007).
[5] A. Connes, J. Math. Phys. (N.Y.) **41**, 3832 (2000).
[6] A. Connes, *Noncommutative Geometry* (Academic Press, New York, 1994).
[7] J. M. Overduin and A. Hamna, arXiv:1607.04580; T. G. Rizzo, J. High Energy Phys. 09 (2005) 036; 11 (2010) 1.
[8] G. Preparata and S.-S. Xue, Phys. Lett. B **264**, 35 (1991).
[9] S. Cacciatori, G. Preparata, S. Rovelli, I. Spagnolatti, and S.-S. Xue, Phys. Lett. B **427**, 254 (1998).
[10] G. Preparata, R. Rovelli, and S.-S. Xue, Gen. Relativ. Gravit. **32**, 1859 (2000).
[11] S.-S. Xue, Phys. Rev. D **82**, 064039 (2010).
[12] M. Zarei, E. Bavarsad, M. Haghighat, I. Motie, R. Mohammadi, and Z. Rezaei, Phys. Rev. D **81**, 084035 (2010).
[13] I. Motie and S.-S. Xue, Int. J. Mod. Phys. A **27**, 1250104 (2012).
[14] T. Jacobson, S. Liberati, and D. Mattingly, Ann. Phys. (N.Y.) **321**, 150 (2006).
[15] S. Liberati and L. Maccione, Annu. Rev. Nucl. Part. Sci. **59**, 245 (2009).
[16] D. Mattingly, Living Rev. Relativ. **8**, 5 (2005).
[17] K. Greisen, Phys. Rev. Lett. **16**, 748 (1966).
[18] M. Takeda *et al.* (AGASA Collaboration), Phys. Rev. Lett. **81**, 1163 (1998).
[19] F. Krennrich *et al.*, Astrophys. J. **560**, L45 (2001).
[20] E. E. Antonov *et al.*, Pis'ma Zh. Eksp. Teor. Fiz. **73**, 506 (2001).
[21] H. Sato, arXiv:astro-ph/0005218.
[22] S. R. Coleman and S. L. Glashow, Phys. Rev. D **59**, 116008 (1999).
[23] R. H. Brandenberger and J. Martin, Int. J. Mod. Phys. A **17**, 3663 (2002); R. H. Brandenberger and J. Martin, Phys. Rev. D **71**, 023504 (2005).
[24] R. Easther, B. R. Greene, W. H. Kinney, and G. Shiu, Phys. Rev. D **64**, 103502 (2001).
[25] A. A. Starobinsky, JETP Lett. **73**, 371 (2001).
[26] J. Martin and R. H. Brandenberger, Phys. Rev. D **65**, 103514 (2002); **68**, 063513 (2003).
[27] O. Bertolami, Classical Quantum Gravity **14**, 2785 (1997).
[28] O. Bertolami, R. Lehnert, R. Potting, and A. Ribeiro, Phys. Rev. D **69**, 083513 (2004).
[29] N. D. Birrell and P. C. W. Davies, *Quantum Fields in Curved Space* (Cambridge University Press, Cambridge, England, 1982).
[30] E. Khajeh, N. Khosravi, and H. Salehi, Phys. Lett. B **652**, 217 (2007).
[31] N. Khosravi, Gen. Relativ. Gravit. **43**, 1417 (2011).
[32] C. Kiefer and D. Polarski, Adv. Sci. Lett. **2**, 164 (2009).
[33] Y. Nambu and Y. Ohsumi, Phys. Rev. D **84**, 044028 (2011).
[34] L. Bombelli, R. K. Koul, J. Lee, and R. D. Sorkin, Phys. Rev. D **34**, 373 (1986).
[35] S. Mukohyama, M. Seriu, and H. Kodama, Phys. Rev. D **55**, 7666 (1997).
[36] H. Terashima, Phys. Rev. D **61**, 104016 (2000).
[37] R. Emparan, J. High Energy Phys. 06 (2006) 012.
[38] P. Lévay, Phys. Rev. D **75**, 024024 (2007).
[39] M. Cadoni, Phys. Lett. B **653**, 434 (2007).
[40] S.-Y. Lin and B. L. Hu, Classical Quantum Gravity **25**, 154004 (2008).
[41] A. Fabbri and J. Navarro-Salas, *Modeling Black Hole Evaporation* (World Scientific, Singapore, 2005).
[42] D. Ahn, Y. Moon, R. Mann, and I. Fuentes-Schuller, J. High Energy Phys. 08 (2008) 062.
[43] G. T. Horowitz and J. Maldacena, J. High Energy Phys. 04 (2004) 008.
[44] D. Gottesman and J. Preskill, J. High Energy Phys. 04 (2004) 026.
[45] S. Lloyd, Phys. Rev. Lett. **96**, 061302 (2006).
[46] D. Ahn, Phys. Rev. D **74**, 084010 (2006).
[47] G. Adesso and I. Fuentes-Schuller, Quantum Inf. Comput. **76**, 0657 (2009).
[48] E. Martín-Martínez, L. J. Garay, and J. León, Phys. Rev. D **82**, 064006 (2010).
[49] X.-H. Ge and S. P. Kim, Classical Quantum Gravity **25**, 075011 (2008).
[50] Q. Pan and J. Jing, Phys. Rev. D **78**, 065015 (2008).
[51] D. Ahn and M. Kim, Phys. Lett. A **366**, 202 (2007).
[52] D. R. Terno, J. Phys. Conf. Ser. **33**, 469 (2006).
[53] E. R. Livine and D. R. Terno, Phys. Rev. D **75**, 084001 (2007).

[54] J. L. Ball, I. Fuentes-Schuller, and F. P. Schuller, Phys. Lett. A **359**, 550 (2006).
[55] I. Fuentes, R. B. Mann, E. Martín-Martínez, and S. Moradi, Phys. Rev. D **82**, 045030 (2010).
[56] E. Martín-Martínez and N. C. Menicucci, Classical Quantum Gravity **29**, 224003 (2012).
[57] E. Martín-Martínez and N. C. Menicucci, Classical Quantum Gravity **31**, 214001 (2014).
[58] E. Martín-Martínez, A. R. H. Smith, and D. R. Terno, Phys. Rev. D **93**, 044001 (2016).
[59] Z. Ebadi and B. Mirza, Ann. Phys. (Amsterdam) **351**, 363 (2014).
[60] Z. Ebadi and B. Mirza, Int. J. Mod. Phys. A **30**, 1550031 (2015).
[61] H. Mohammadzadeh, Z. Ebadi, H. Mehri-Dehnavi, B. Mirza, and R. Rahimi, Quantum Inf. Process. **14**, 4787 (2015).
[62] R. Pierini, S. Moradi, and S. Mancini, Int. J. Theor. Phys. **55**, 3059 (2016).
[63] R. B. Mann and T. C. Ralph, Classical Quantum Gravity **29**, 220301 (2012).
[64] D. M. T. Benincasa, L. Borsten, M. Buck, and F. Dowker, Classical Quantum Gravity **31**, 075007 (2014).
[65] P. M. Alsing and G. J. Milburn, Phys. Rev. Lett. **91**, 180404 (2003).
[66] P. M. Alsing, I. Fuentes-Schuller, R. B. Mann, and T. E. Tessier, Phys. Rev. A **74**, 032326 (2006).
[67] G. Adesso, I. Fuentes-Schuller, and M. Ericsson, Phys. Rev. A **76**, 062112 (2007).
[68] H. Mehri-Dehnavi, R. Rahimi, H. Mohammadzadeh, Z. Ebadi, and B. Mirza, Quantum Inf. Process. **14**, 1025 (2015).
[69] A. Helder, G. de Souza, P. Mansfield, and M. Sampaio, Europhys. Lett. **111**, 60001 (2015).
[70] R. Müller and C. O. Lousto, Phys. Rev. D **52**, 4512 (1995).
[71] M. Han, S. J. Olson, and J. P. Dowling, Phys. Rev. A **78**, 022302 (2008).
[72] P. M. Alsing and I. Fuentes, Classical Quantum Gravity **29**, 224001 (2012).
[73] N. Liu, J. Goold, I. Fuentes, V. Vedral, K. Modi, and D. E. Bruschi, Classical Quantum Gravity **33**, 035003 (2016).
[74] M. Farahmand, H. Mohammadzadeh, and H. Mehri-Dehnavi, Int. J. Mod. Phys. A **A32**, 1750066 (2017).
[75] S.-S. Xue, Phys. Lett. B **706**, 213 (2011).
[76] G. Amelino-Camelia, Living Rev. Relativ. **16**, 5 (2013).
[77] V. Mukhanov, *Physical Foundations of Cosmology* (Cambridge University Press, Cambridge, England, 2005).
[78] V. Vedral, *Introduction to Quantum Information Science* (Oxford University Press, New York, 2006).
[79] N. D. Birrell, Proc. R. Soc. A **367**, 123 (1979).
[80] P. M. Alsing, D. H. McMahon, and G. J. Milburn, J. Opt. B **6**, S834 (2004).
[81] B. Yurke and M. Potasek, Phys. Rev. A **36**, 3464 (1987).
[82] C. Gerry and P. Knight, *Introductory Quantum Optics* (Cambridge University Press, Cambridge, England, 2005).
[83] M. Campisi, P. Hänggi, and P. Talkner, Rev. Mod. Phys. **83**, 771 (2011).
[84] H. Tasaki, arXiv:cond-mat/0009244.
[85] D. J. Evans, E. G. D. Cohen, and G. P. Morriss, Phys. Rev. Lett. **71**, 2401 (1993).
[86] G. E. Crooks, Phys. Rev. E **60**, 2721 (1999).
[87] C. Kittel and F. H. Donald, Am. J. Phys. **35**, 547 (1967).
[88] B. Reznik, A. Retzker, and J. Silman, Phys. Rev. A **71**, 042104 (2005).
[89] G. Ver Steeg and N. C. Menicucci, Phys. Rev. D **79**, 044027 (2009).
[90] Y. Nambu, Phys. Rev. D **78**, 044023 (2008).
[91] Y. Nambu, Entropy **15**, 1847 (2013).
[92] R. Simon, Phys. Rev. Lett. **84**, 2726 (2000).
[93] W. G. Unruh, Phys. Rev. Lett. **46**, 1351 (1981).
[94] H. V. Peiris *et al.*, Astrophys. J. Suppl. Ser. **148**, 213 (2003).
[95] P. G. Kwiat, K. Mattle, H. Weinfurter, A. Zeilinger, A. V. Sergienko, and Y. Shih, Phys. Rev. Lett. **75**, 4337 (1995).
[96] A. Aspect, P. Grangier, and G. Roger, Phys. Rev. Lett. **49**, 91 (1982).
[97] Y. Fukuda *et al.*, Phys. Rev. Lett. **81**, 1562 (1998).
[98] G. Mangano, G. Miele, S. Pastor, T. Pinto, O. Pisanti, and P. D. Serpico, Nucl. Phys. **B729**, 221 (2005).
[99] R. Trotta and A. Melchiorri, Phys. Rev. Lett. **95**, 011305 (2005).
[100] M. Longair, *The Cosmic Century: A History of Astrophysics and Cosmology* (Cambridge University Press, Cambridge, England, 2006).
[101] C. Barceló, S. Liberati, and M. Visser, Living Rev. Relativ. **8**, 12 (2005).
[102] P. O. Fedichev and U. R. Fischer, Phys. Rev. Lett. **91**, 240407 (2003).
[103] P. O. Fedichev and U. R. Fischer, Phys. Rev. D **69**, 064021 (2004).
[104] M. Uhlmann, Y. Xu, and R. Schützhold, New J. Phys. **7**, 248 (2005).
[105] P. Jain, S. Weinfurtner, M. Visser, and C. W. Gardiner, Phys. Rev. A **76**, 0336169 (2007).
[106] R. Schützhold, M. Uhlmann, L. Petersen, H. Schmitz, A. Friedenauer, and T. Schatz, Phys. Rev. Lett. **99**, 201301 (2007).
[107] R. Schutzhold, Adv. Sci. Lett. **2**, 121 (2009).
[108] G. E. Volovik, *The Universe in a Helium Droplet* (Oxford University Press, Oxford, 2003).
[109] M. delRey, D. Porras, and E. Martín-Martínez, Phys. Rev. A **85**, 022511 (2012).
[110] A. Ashtekar and B. Gupt, Classical Quantum Gravity **34**, 014002 (2017); M. Arzano and G. Calcagni, Phys. Rev. D **93**, 124065 (2016); G. K. Chakravarty, G. Lambiase, and S. Mohanty, arXiv:1607.06325; D. A. Quinones, T. Oniga, B. T. Varcoe, and C. H. T. Wang, arXiv:1702.03905.
[111] It is noteworthy that experimental searches for Lorentz violation have been exploited to make new constraints on the components of spacetime torsion; see, e.g., [112].
[112] V. A. Kostelecky, N. Russell, and J. D. Tasson, Phys. Rev. Lett. **100**, 111102 (2008).
[113] C. D. Carone, M. Sher, and M. Vanderhaeghen, Phys. Rev. D **74**, 077901 (2006).

[114] C. Quercellini, L. Amendola, A. Balbi, P. Cabella, and M. Quartin, Phys. Rep. **521**, 95 (2012).

[115] D. H. Weinberg, M. J. Mortonson, D. J. Eisenstein, C. Hirata, A. G. Riess, and E. Rozo, Phys. Rep. **530**, 87 (2013).

[116] G. Gubitosi, L. Pagano, G. Amelino-Camelia, A. Melchiorri, and A. Cooray, J. Cosmol. Astropart. Phys. 08 (2009) 021.

[117] R. Pierini, Sh. Moradiy, and S. Mancini, arXiv:1606.03005v1.